Proceedings of GT2005
ASME Turbo Expo 2005: Power for Land, Sea and Air
June 6-9, 2005, Reno-Tahoe, Nevada, USA

GT2005-68151

THE INTERACTION OF TURBINE INTER-PLATFORM LEAKAGE FLOW WITH THE MAINSTREAM FLOW

Kevin Reid[*], **John Denton, Graham Pullan, Eric Curtis, John Longley**
Whittle Laboratory
Department of Engineering
University of Cambridge
United Kingdom
Email: kjr33@eng.cam.ac.uk

ABSTRACT

Individual nozzle guide vanes (NGVs) in modern aero engines are often cast as a single piece with integral hub and casing endwalls. When in operation there is a leakage flow through the chord-wise inter-platform gaps. An investigation into the effect of this leakage flow on turbine performance is presented. Efficiency measurements and NGV exit area traverse data from a low speed research turbine are reported. Tests show that this leakage flow can have a significant impact on turbine performance, but that below a threshold leakage fraction this penalty does not rise with increasing leakage flow rate. The effect of various seal clearances are also investigated. Results from steady-state simulations using a three-dimensional multiblock RANS solver are presented with particular emphasis paid to the physics of the mainstream/leakage interaction and the loss generation.

NOMENCLATURE

Variables:

c_v	specific heat capacity at constant volume
c_p	specific heat capacity at constant pressure
m	massflow
P	pressure
$\dot{s}$	entropy generation rate
T	temperature
T_q	torque
V	velocity
Y_p	NGV Loss Coefficient
ω	rotational speed
ϕ	flow coefficient $= V_{merid2}/U_{mid2}$
γ	specific heat ratio $= \frac{c_p}{c_v}$
η	efficiency
$\underline{\tau}$	shear stress
$\underline{x}$	area averaged x
x	mass averaged x

Subscripts:

br	brake
m	mainstream quantity
merid	meridional
mid	midspan
0	stagnation quantity
s	leakage quantity
st	static quantity
$1,2,3$	downstream of the IGV, NGV and rotor

INTRODUCTION

The stationary vane in many gas turbine engines is cast as a single unit consisting of a blade with integral hub and casing endwalls. These individual units are then joined circumferentially to form a ring of vanes. When the engine is operating, there is in-

[*]Address all correspondence to this author.

evitably a gap along the mating surfaces of the individual stator units. Leakage flow is pumped through this platform gap in order to avoid the ingress of combustion gases into the wheelspace. Chordwise slots can also be found in rotating blade rows, however this study was concerned exclusively with stationary vanes. To the authors' knowledge, the interaction of this leakage flow and the mainstream flow has not been previously reported in the open literature.

Aunapu et. al. [1] investigated the use of hub endwall jets to modify secondary flow in a cascade of turbine vanes. They modified the secondary flow both through the use of jets and through the use of a stationary fence. In both cases, the flow control resulted in the pressure side leg of the horseshoe vortex being deflected away from the suction surface of the adjacent blade, but did not affect the strength of the vortex. Compared with a baseline case, the fence resulted in a loss reduction of 10%. In order to achieve the same change in the path of the passage vortex as was observed in the fence study, approximately 2% of the mainstream flow was blown through the jets which were distributed over 44% of the chord. At this condition, the jets resulted in losses 30% greater than those observed in the baseline case. This study indicates that a leakage flow along the hub surface of a turbine passage can have a significant affect on performance.

The effect of the leakage flow through the inter-platform gaps on the hub surface of a low speed axial flow turbine is presented in this study. A detailed understanding of the experimental results is obtained through three dimensional steady-state CFD simulations.

EXPERIMENTAL SETUP

The experimental results collected in this paper were obtained from a full scale, low speed axial flow turbine. The same facility is described in a past ASME paper [2], however major modifications to both the annulus and the blading have been made since this time and the current configuration is briefly described here. A schematic of the facility is shown in Figure 1. The machine is characterized by a significant radius change through the stage as well as by a low aspect ratio, low turning vane. Air was drawn through the turbine by a fan that was mounted on a separate shaft and driven by a 200kW electric motor (not shown in schematic). An eddy current dynamometer controlled the shaft speed at 1100RPM.

Inlet Guide Vanes (IGV's) were used to generate an inlet yaw angle distribution representative of engine conditions. An engine representative inlet stagnation pressure profile was generated using a wire gauze upstream of the IGV's and by selectively obstructing the flow at both the hub and the casing at the same axial location as the wire gauze.

Figure 1 shows the piping arrangement that was used to introduce leakage flow into the wheelspace of the rig. Leakage air was supplied by an industrial vacuum cleaner driven by a 2.4 kW electric motor (not shown in schematic). The mass flow of the secondary air was measured before it entered the rig in a long section of straight pipe using pitot and static tappings as outlined by Ower and Pankhurst [3]. The secondary air was introduced into a sealed plenum through perforations in the supply pipe. Due to the low fluid velocity in the plenum, the total pressure of the leakage flow was taken as the static pressure. The total temperature of the leakage flow was measured in the supply pipe.

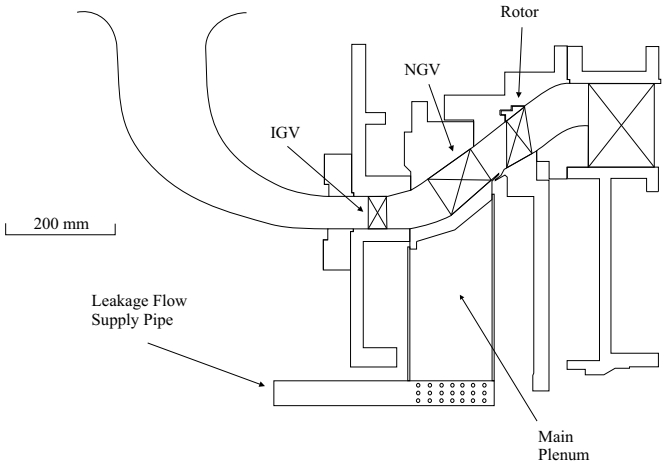

Figure 1. Overview of the Experimental Apparatus

The temperature drop across the turbine is small. This means that small uncertainties in the temperature measurement lead to high overall uncertainties in the efficiency. For this reason, the work done by the turbine was determined by the shaft torque and speed. The efficiency definition also needs to account for the potential work of the leakage flow. The efficiency of the rig was therefore defined as:

$$\eta_{br} = \frac{T_q \omega}{m_m c_p T_{01m}\left(1-\left(\frac{\overline{P_{03}}}{\overline{P_{01m}}}\right)^{\frac{\gamma-1}{\gamma}}\right) + m_s c_p T_{01s}\left(1-\left(\frac{\overline{P_{03}}}{P_{01s}}\right)^{\frac{\gamma-1}{\gamma}}\right)} \quad (1)$$

The inlet total pressure was determined by a set of 10 pitot tubes located downstream of the IGV's. These probes were equispaced around the circumference at various radii (from 6% span to 96% span), and circumferential variations were measured by traversing them all over one IGV pitch. The exit total pressure was determined by a set of 10 self aligning pitot tubes located downstream of the rotor at various radii (from 5% span to 95% span), with an area average determined by traversing the probes over one NGV pitch. The torque was measured by a load cell which was connected through a lever arm to the dynamometer. The rotational speed was measured by an optical trigger located on the turbine shaft. The inlet total temperature was measured

by the arithmetic average of 6 thermocouples located in the bell mouth inlet. At each condition investigated in this paper, the efficiency was measured four times and the average value of these measurements is reported. The scatter within these four measurements was never observed to be greater than $\pm 0.10\%$ even when measurements were conducted over several days. A detailed uncertainty analysis using the method outlined in [4] also resulted in a repeatability uncertainty of $\pm 0.10\%$.

Area traverses could be conducted downstream of each blade row using a pneumatic five hole probe as shown in Figure 2. All traverses reported in this work were completed at traverse planes 2 and 3. An NGV loss coefficient can be determined by conducting area traverses both upstream and downstream of the stator. Again, this loss coefficient must account for the potential work of the leakage flow and is defined as:

$$Y_p = \frac{[m_m \overline{\overline{P_{01m}}} + m_s P_{01s}] - (m_m + m_s)\overline{\overline{P_{02}}}}{(m_m + m_s)[\overline{\overline{P_{02}}} - \overline{P_{st2}}]} \qquad (2)$$

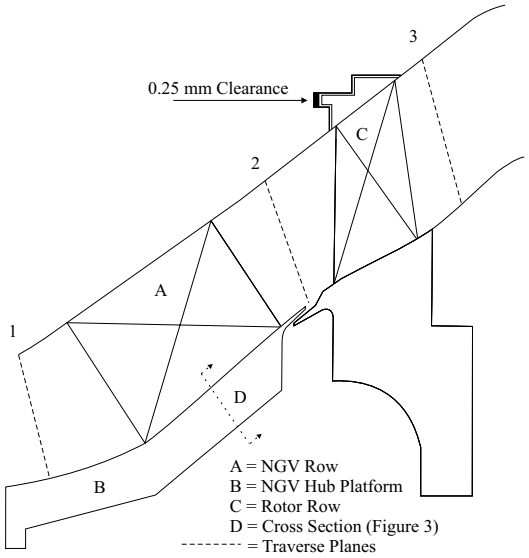

Figure 2. Detail of the Experimental Turbine Stage

Figure 3 shows the location of the slot in the blade to blade plane, along with a cross section of the leakage arrangement in a plane perpendicular to the slot axis (cross section plane illustrated in Figure 2). The terms slot, plenum and strip seal will be used often in the body of the paper and it is important to note their definitions from Figure 3. The plenum is 25mm deep and then exhausts into the larger plenum shown in Figure 1.

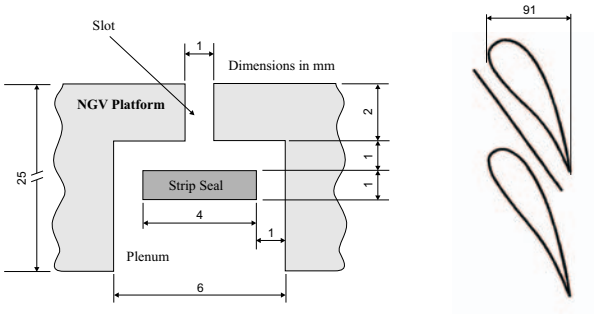

Figure 3. Detail of the Slot Location and Datum Leakage Arrangement

NUMERICAL CODE

The numerical calculations were completed using TBLOCK, a Reynolds Averaged Navier Stokes (RANS) solver written by John Denton. This code is an extension of Denton's Multip [5] and Unstrest [6] turbomachinery codes but can be used to solve the flow in both the main blade path and any secondary gas paths. This is achieved using a multi-block approach where complex geometries are divided into a series of blocks, each of which is solved as a separate structured grid. Information is transferred between the various blocks via user defined patches. If the meshes on the two adjacent patches are identical, the flow variables are transferred directly from block to block.

TBLOCK is a finite volume code which uses the 'Scree' scheme for time advancement [6]. Turbulence is modelled using a mixing length model with wall functions used to determine the surface skin friction. Laminar/turbulent transition can be modelled by assuming laminar boundary layers and viscosity until a specified location with turbulent boundary layers and viscosity downstream of this location. With a mixing plane at the interface between blade rows, the code is accelerated to a steady state solution using multigrid and spatially varied time steps. By using dual time stepping, these same convergence acceleration techniques are also employed when the code is run in unsteady mode with a sliding interface between the blade rows.

The CFD geometry modelled the full annulus stage (NGV and Rotor) using a mixing plane approach. The slot, strip seal and plenum arrangement shown in Figure 3 was also modelled. It was impractical to model the entire large plenum shown in Figure 1, therefore an additional 12mm wide $\times$ 25mm deep plenum was included beneath the 6mm wide plenum, Figure 4. This ensured that any mainstream flow entering the plenum was not influenced by the leakage flow inlet boundary condition. Unless stated otherwise, all boundary layers in this work were assumed to be fully turbulent.

Entropy is the best quantity to use when investigating loss in turbomachines [7]. Entropy is a convected quantity. This means that the entropy present at any particular location in a machine

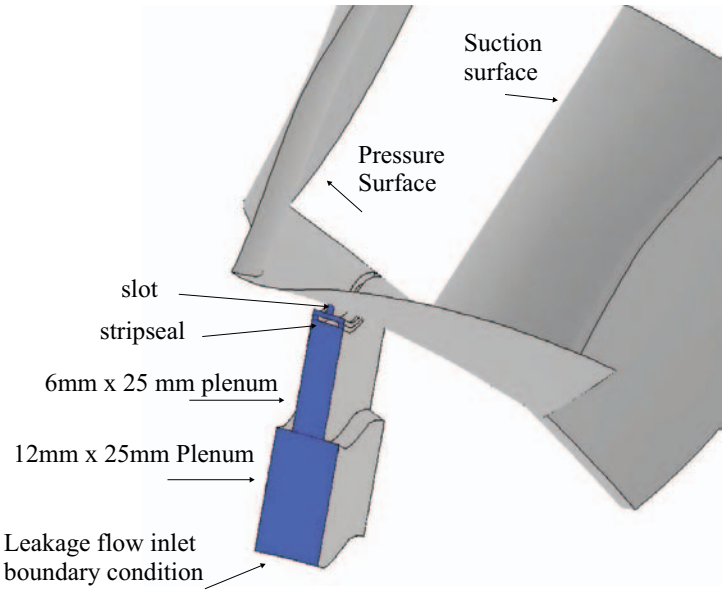

Figure 4. CFD Geometry (NGV Passage and Slot/Seal/Plenum Arrangement)

could have been created at that location or it could have been created upstream and convected into the downstream location. In order to clearly identify areas of high loss, entropy generation rates [8] have been added to TBLOCK. The rate of entropy production per unit volume is given by:

$$\dot{s} = \frac{1}{T}\tau_{ik}\frac{\partial V_i}{\partial x_k} + \frac{k}{T^2}\frac{\partial T}{\partial x_i}\frac{\partial T}{\partial x_i} \tag{3}$$

RESULTS

Verification of CFD

Figure 5 shows a comparison of experimental and numerical data of the pitchwise averaged meridional yaw angle distribution on traverse plane 2 with the inter-platform slot taped over. The agreement between CFD and experiment is within 2° over the entire span.

Figure 6 shows a comparison of experimental and numerical data of the pitchwise averaged meridional yaw angle distribution on traverse plane 2 with no net leakage through the inter-platform slot. Again the agreement between CFD and experiment is within 2° over the entire span. The CFD is also following the same trend over the bottom 20% of the span as the experimental results when the tape is removed from the slot. It is interesting to note that the agreement between CFD and experiment is better for the no net leakage configuration than it is for the taped over configuration. The reason for this is not clear. The

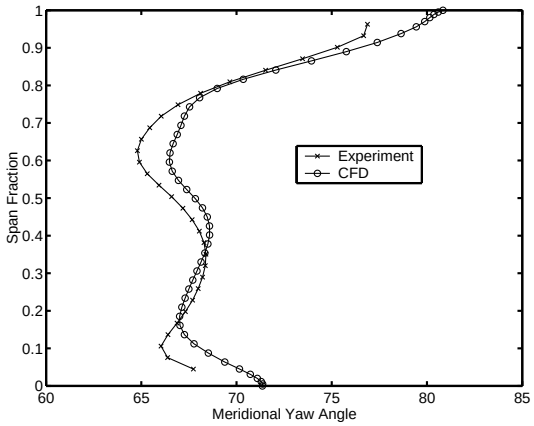

Figure 5. Comparison of Experiment and CFD With Slot Taped Over - Meridional Yaw Angle at Traverse Plane 2

CFD also predicts the efficiency of the no-slot case within 0.5% of the experimental result.

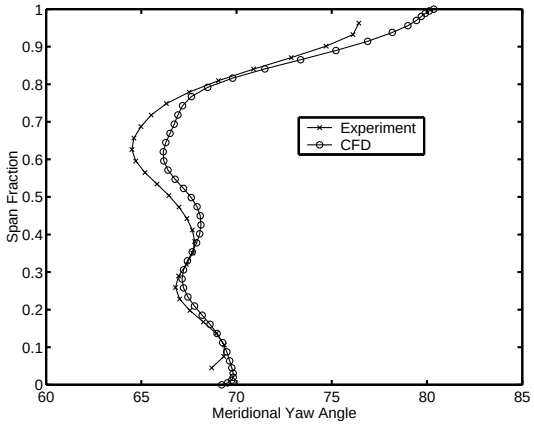

Figure 6. Comparison of Experiment and CFD With No Net Leakage - Meridional Yaw Angle at Traverse Plane 2

Effect of Leakage Mass Flow

Figure 7 shows the experimental normalized brake efficiency with increasing leakage mass flow. The efficiencies are normalized by the efficiency of the rig when the slot is taped over. It is clear that there is an approximately 1.2% drop in efficiency when the slot is opened, even when there is no applied leakage flow. It is also clear that increasing the leakage flow rate up to 1.5% causes no significant change in the efficiency. Figure 8 shows the normalized turbine efficiency obtained from CFD

over the same range of leakage fractions. Again it is evident that it is the presence of the slot that is causing the loss of efficiency and that increasing the mass flow has little effect.

Figure 9 shows the mass flow into and out of the slots obtained from the CFD solutions at various leakage mass fractions. The data has been normalized so that any change from zero indicates that mass is either entering (+ve) or leaving (-ve) the main blade passage. With no net flow, approximately 1.25% of the mainstream flow is leaving the main annulus along the front 50% of the slot and then re-entering along the rear 50% of the slot. As the leakage flow is increased, less fluid leaves the mainstream annulus, but the net exchange of fluid between the plenum and the mainstream remains constant at approximately 1.5%. From this result, one would be tempted to conclude that the addition of leakage flow does not lead to a significantly higher efficiency penalty because the quantity of flow being re-introduced into the annulus from the plenum is approximately constant in all cases. In the next section, entropy generation rates will be used to show that the true picture is more complicated.

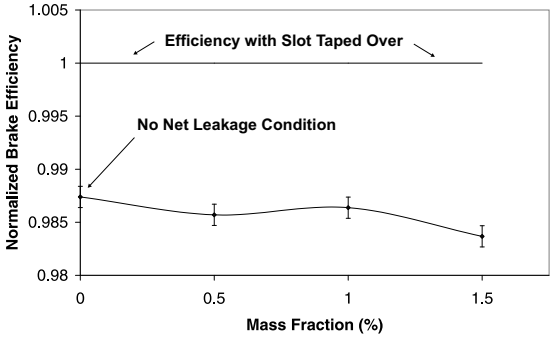

Figure 7. Normalized Brake Efficiency With Varying Mass Fraction - Experimental

Figure 10 shows a comparison of the pitchwise-averaged loss coefficients for various leakage flows. These results were obtained from five hole probe traverses and are independent of the efficiency results. They serve to reinforce the fact that increasing leakage flow does not create significantly more loss.

Figure 11 shows a comparison of experimental loss contours between a no leakage case (slot taped over) and a no net leakage case. The increased area of loss due to the mixing of the leakage flow and the mainstream is evident on the bottom left hand corner of Figure 11b. The leakage flow has also altered the structure of the wake.

Figure 12 shows that the flow entering the mainstream annulus along the rear half of the slot creates an air curtain that inhibits the secondary flow from sweeping along the hub endwall. It is

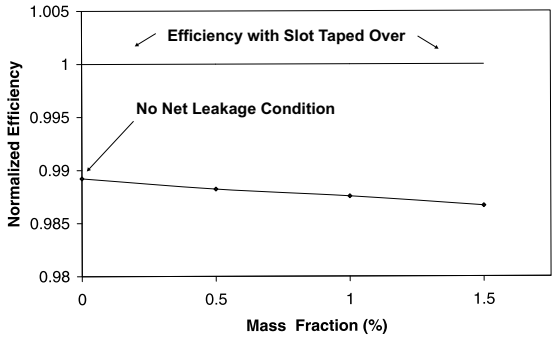

Figure 8. Normalized Efficiency With Varying Mass Fraction - Computational

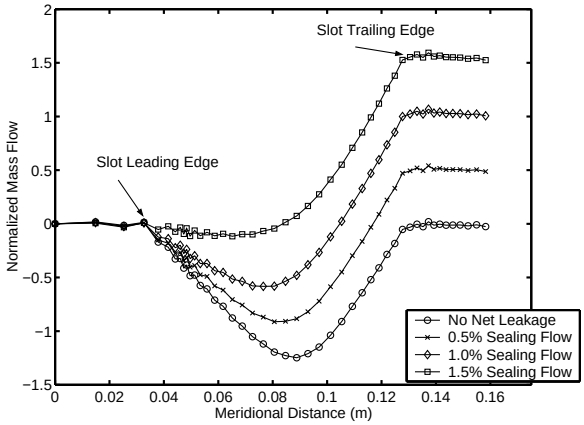

Figure 9. Mass Fraction of Fluid Exchanged Between the Mainstream and the Plenum - Normalized Mass Flow = $\frac{m_{merid} - m_{inlet}}{m_{inlet}}$ - (Every Third Point Shown for Clarity)

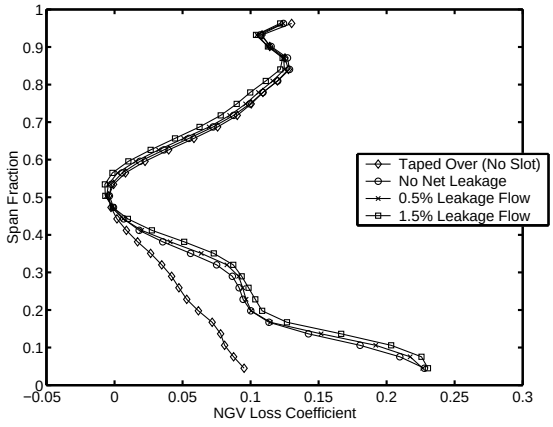

Figure 10. Measured NGV Loss Coefficient With Varying Leakage Flow

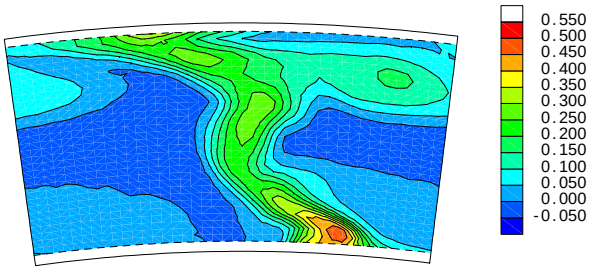

(a) No Leakage

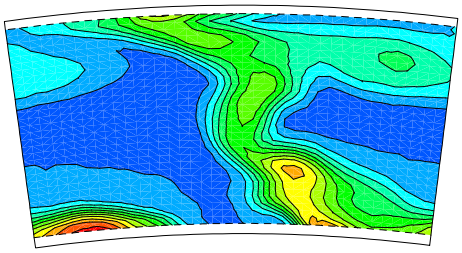

(b) No Net Leakage

Figure 11. Measured NGV Loss Coefficient

this blockage that results in the reduction of loss in the wake near the hub of Figure 11b. The CFD NGV loss coefficient contours (not shown) do not show the area of increased loss at 30% span in the wake in the no net leakage case. However, this is either boundary layer fluid that has been deflected up the span due to the air curtain, or is mixing loss created through the introduction of the leakage flow.

Five hole probe traverses were also conducted downstream of the rotor and the pitchwise averaged relative meridional yaw angle is plotted in Figure 13. The flow downstream of the rotor is little affected by the leakage flow and will not impact significantly on the flow in downstream stages.

Annulus Losses vs. Plenum Losses

CFD calculations along with entropy generation rates were used to compare the magnitude of the losses created by the mixing of the leakage flow when it re-enters the mainstream and the subsequent effect that this has on secondary flow, to the losses generated in the slot and plenum geometry, Figure 14. The entropy generation rates defined by equation (3) are calculated per cell in the CFD calculation. To obtain the curves shown in Figure 14 these cell values are summed at each meridional location, and these totals are then summed up along the length of the machine. The value at a given meridional location represents the total rate of entropy generation in the volume preceding that location. This

(a) No Leakage

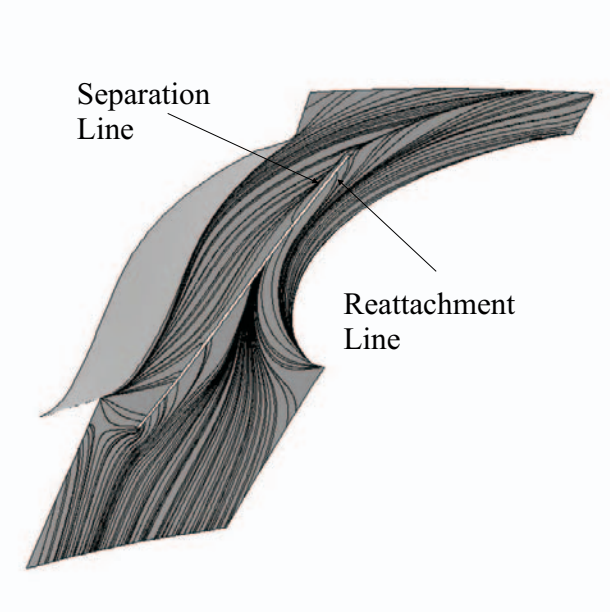

(b) No Net Leakage

Figure 12. Computational NGV Hub Surface Streamlines

quantity will be referred to as the cumulative entropy generation rate. The 'plenum' lines represent the cumulative entropy generation rate in the slot/strip-seal/plenum geometry at each meridional location. The 'annulus' lines represent the difference in the cumulative entropy generation rate in the annulus for a CFD calculation including a plenum and slot/strip-seal arrangement, and an annulus only calculation. The fact that these lines drop below

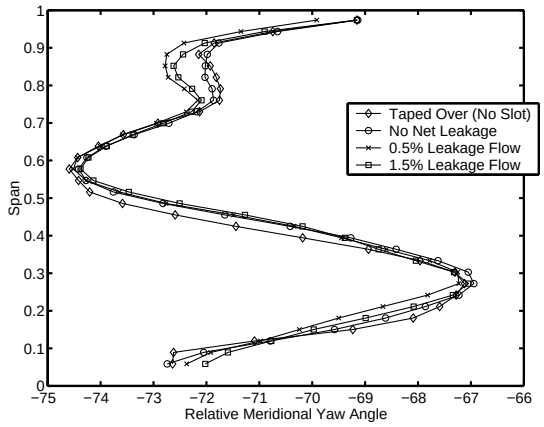

Figure 13. Relative Meridional Yaw Angle Downstream of the Rotor

zero entropy generation rate between x = 0.05 and x = 0.1 indicates that there is actually less loss generated in the annulus along the forward part of the slot in the calculation which included the slot/stripseal/plenum arrangement.

The key result from this plot is that the plenum losses are greater in the no net leakage case than they are with 1.5% leakage flow, but that the annulus mixing and secondary flow losses are greater with 1.5% leakage flow. This shows that the nearly constant efficiency reported in Figure 7 is due to the balance of losses occurring in the plenum and annulus, and is not due solely to the fact that a similar mass fraction is being injected into the mainstream flow along the trailing edge of the slot in both scenarios.

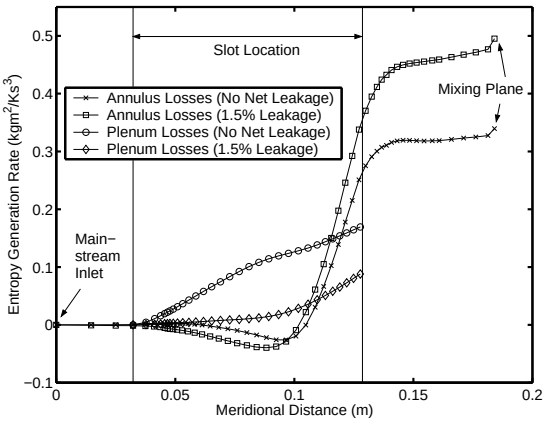

Figure 14. Comparison of the Cumulative Entropy Generation Rates in the Annulus and in the Plenum (No Net Leakage)

Figure 15 shows the variation in cumulative entropy generation rate along the length of the 6 ‘blocks’ shown on the right hand side of the plot for all leakage fractions. With no net leakage, the majority of the loss is occurring in block 2, the 6mm x 25mm plenum. A more detailed investigation of the flow-field shows that the majority of this loss occurs along the plenum walls and is due to the ingested mainstream fluid. As the leakage fraction is increased, less fluid is ingested into block 2 and subsequently there is less loss.

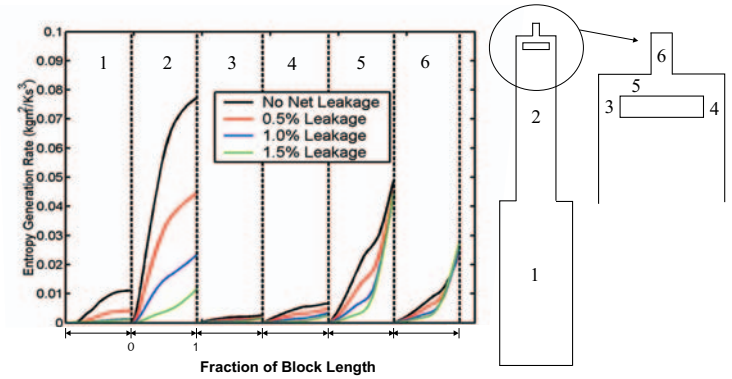

Figure 15. Distribution of the Cumulative Entropy Generation Rate in the Slot/Strip-Seal/Plenum

Blocks 3 and 4 show different amounts of loss. More of the flow leaving the mainstream annulus enters the plenum through block 4 than block 3. This appears to be due to the fact that block 4 is on the side of the plenum that is closest to the suction surface of the blade; the annulus secondary flow is driving more fluid through block 4. It may be possible to capitalize on this preferential movement of the fluid through the slot in order to achieve a better seal.

Effect of Slot Length

Figure 3 shows that the datum slot ends 7mm axially upstream of the trailing edge of the NGV. Calculations were conducted with the slot extended to the trailing edge of the vane and 7mm axially downstream of the vane trailing edge. The resulting change in the annulus mass flow is shown in Figure 16. By extending the slot 14mm axially, an additional 0.4% mass flow is being exchanged with the plenum. This extra 0.4% mass flow leads to a predicted additional 0.6% drop in efficiency, showing that the length of the slot can have a significant effect on the loss.

Due to the geometry of the rig and the presence of the rim seal, it was impractical to conduct experiments to verify these results.

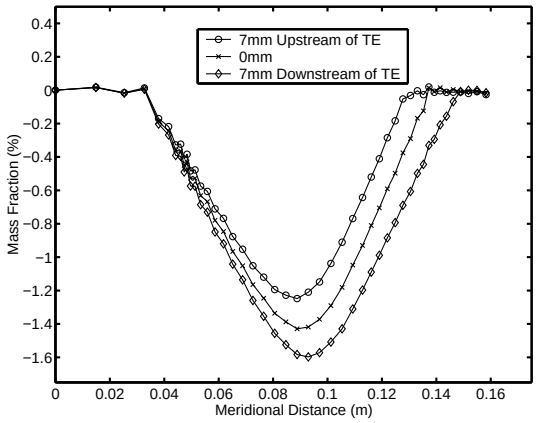

Figure 16. Effect of Slot Length on Mass Flow

Effect of Varying Seal Clearance

The flow through the slot is determined by the pressure gradient along the length of the slot and by the quality of the seal between the plenum and the annulus. Experiments were conducted with various seal clearances to determine the range of efficiency penalty that can be incurred due to the sealing of the plenum. In addition to the datum configuration, three seal clearances were investigated and these are shown in Figure 17 along with the measured efficiency penalty incurred by each. All of these results were obtained with no net flow through the slot. The 0mm clearance shown in Figure 17c did not provide a perfect seal due to variations in the strip seal along its chordwise axis. For this reason, the geometry shown in Figure 17d had a sealing foam placed beneath the strip seal. The largest drop in efficiency due to inter-platform gaps was found to be 1.54% and the smallest drop in efficiency with only a 2mm deep slot was found to be 0.46%. These results are only for a hub slot, there will likely be a similar penalty due to the slot at the casing; these slots could thus be responsible for a $1-3\%$ drop in efficiency.

Figure 18 shows contours of NGV loss coefficient for the foam backed zero clearance case (Figure 17d). Comparing this plot with Figure 11a, it is clear that the slot leads to more loss in the loss core. When there is no large exchange of mass between the plenum and the annulus, it is proposed that the slot flow no longer creates a significant blockage to the secondary flow. Instead the secondary flow incurs more loss as it crosses the slot, which leads to the deeper loss core. Neither the efficiency drop of this geometry nor the increase in the depth of the NGV loss core were predicted well by the CFD. Specifying laminar/turbulent transition to occur halfway along the slot led to no improvement in the agreement between the experiments and CFD. It is possible that improved transition modelling would improve the agreement. The flow in the region of the slot is likely dominated by small scale turbulent mixing, and it is also possible that the mixing length model applied in TBLOCK is unable to model this flow accurately.

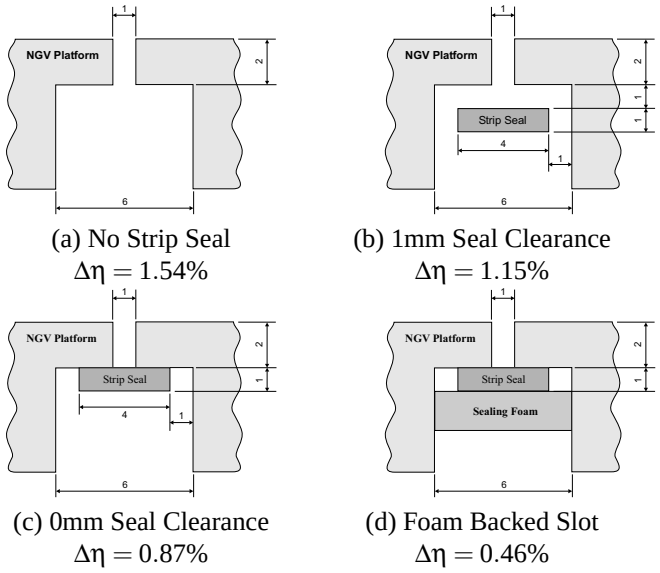

Figure 17. Various Seal Clearances (Dimensions in mm)

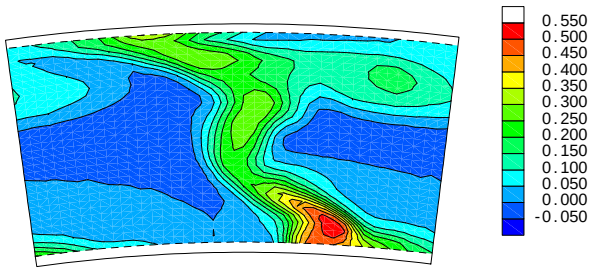

Figure 18. Measured NGV Loss Coefficient With 0mm Clearance and Foam Backing

Without removing platform slots from engines, Figure 17d offers the best case scenario. In engine installations it is likely that these slots would extend along the entire length of the platform and cut through into the rim-seal. As was shown earlier, the length of the slot can have a significant impact on the performance penalty. It was possible to extend the experimental 2mm slot to the trailing edge of the NGV platform, and cut through into the rim seal, as shown in Figure 19.

With the geometry of Figure 17d on the portion of the slot upstream of the extension and with the platform cut through into the rim seal along the extension, an efficiency drop of 0.7% was measured. The small extension of the slot into the rim seal was therefore responsible for a drop of 0.24% over the configuration shown in Figure 17d. This again emphasizes the fact that small changes in the geometry of a turbine can have a relatively large

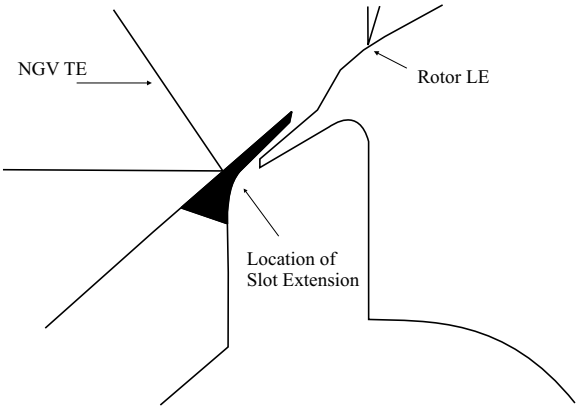

Figure 19. Detail of the Slot Extension

effect on the efficiency.

CONCLUSIONS

This work has investigated the effect of chordwise hub platform slots on the performance of a low speed axial flow turbine. With a 1mm seal clearance, the presence of the slots led to a significant performance penalty even with no net leakage flow. The quality of the seal between the mainstream annulus and the wheelspace was found to be critical with a perfect seal resulting in a 1.08% efficiency improvement over an unsealed slot. Even when perfectly sealed, the presence of a 2mm deep $\times$ 1mm wide slot running along the chord of the blade resulted in a 0.46% drop in efficiency compared with a smooth annulus.

ACKNOWLEDGMENT

The authors would like to acknowledge the assistance of Nick Hooper of the Whittle Laboratory. The financial assistance of the Natural Sciences and Engineering Research Council of Canada, the Edmonton Churchill Society and Rolls-Royce is also gratefully acknowledged

REFERENCES

[1] Aunapu, N., Volino, R., Flack, K., and Stoddard, R., 2000. "Secondary Flow Measurements in a Turbine Passage With Endwall Flow Modification". *ASME 2000-GT-0212* .

[2] Pullan, G., Denton, J., and Dunkley, M., 2003. "An Experimental and Computational Study of the Formation of a Streamwise Shed Vortex in a Turbine Stage". *ASME Journal of Turbomachinery* , pp. 291,297.

[3] Ower, E., and Pankhurst, R., 1965. *Measurement of Air Flow*, Fourth ed. Pergamon.

[4] Beckwith, T., Marangoni, R., and Lienhard, J., 1993. *Mechanical Measurements*, Fifth ed. Addison Wesley Publishing.

[5] Denton, J. D., 1990. "The Calculation of Three Dimensional Viscous Flow Through Multistage Turbomachines". *ASME 90-GT-19* .

[6] Pullan, G., and Denton, J., 2003. "Numerical Simulations of Vortex-Turbine Blade Interaction". *Conference Proceedings: 5th European Conference on Turbomachinery: Fluid Dynamics and Thermodynamics* .

[7] Denton, J. D., 1993. "Loss Mechanisms in Turbomachines". *ASME Journal of Turbomachinery*, **115** , pp. 621–656.

[8] Dawes, W., 1987. "Application of a Three Dimensional Viscous Compressible Flow Solver to a High Speed Centrifugal Compressor Rotor - Secondary Flow and Loss Generation". *IMECHE Paper C261/87* .